Unsteady Aerodynamics of Offshore Floating Wind Turbines Using Free Vortex Wake Model

Qi Qi, Nigel Barltrop
Naval Architecture Ocean and Marine Engineering, University of Strathclyde
Glasgow, UK

ABSTRACT

Among the offshore floating wind turbine software packs, the blade element momentum theory (BEM) and generalized dynamic wake (GDW) model are widely used. A free vortex wake model has been coupled to FAST v7 to do a comparative dynamic analysis between using the BEM theory and GDW method on offshore floating wind turbine. The verification test on the free-wake model has been performed according to the NREL VI experiment in steady and yaw conditions. To analyze the unsteady aerodynamics of floating wind turbine, the OC3 spar type wind turbine has been used to do simulations. The global performances on both the rotor and the platform and their interactions are shown and discussed.

KEY WORDS: Offshore floating wind turbine; vortex model; coupled analysis; numerical simulation

INTRODUCTION

To produce more wind power and cut the offshore wind costs a floating wind turbine is a suitable type to be designed and constructed for its capability in deep water area with plentiful wind source. When the wind turbine is oscillating in 6 DOFs, it encounters unsteadiness which makes the flow complex. The BEM method used for steady state may not be reliable to solve the problem. Even for the onshore wind turbine, the wind turbine may be working in yaw condition, shear wind and some other dynamic inflow conditions. Free vortex wake model can represent the strengths and locations of the vortex filaments in a time-marching procedure. The induced velocity on blades and flow field can be obtained via Biot-Savart low.

In the past two decades, many researchers have developed their own codes using the free-wake theory. The software AWSM from ECN provided accurate result in the simulation of wind turbines (van Garrel, 2003). Researchers in the University of Glasgow developed a prescribed-wake code (Wang, 1999) for wind turbines which has been validated according to the NREL UAE test. An inverse free-wake model was developed to help modifying the BEM method (Sant, 2007). The platform velocities were introduced onto the wind turbine as induced velocities (Sebastian, 2012). It made the free-wake model possible to analyse the floating wind turbine with input platform velocities and motions.

The aim of this paper is to investigate the unsteady behavior of floating wind turbines using a free-wake model together with commonly used BEM and GDW theories. Nearly all OC3 and OC4 participated codes are using BEM or GDW theory as the aerodynamic simulator except hydro-GAST from NTUA (Robertson et al., 2014). The hydro-GAST can use free-wake model to calculate loads. The free wake model AWSM has been interfaced into the multi-body simulation code SIMPACK (Bülk, 2012). The comparison on floating wind turbine extreme pitching motions has been done by Dr Matha (Matha et al., 2013) through BEM, free wake and CFD models with prescribed platform motions. The floating wind turbine has been modeled in a single two-phase URANS CFD solver with quasi-static mooring lines (Quallen et al., 2014). In the above two papers discrepancies on rotor power by BEM theory and other dynamic models are found.

A prescribed wake model has been interfaced into FAST v6 by Prof Hugh Currin (Currin, 2007). This prescribed wake model in FAST v6 was validated according to NREL VI test. Prof Hugh Currin updated the prescribed wake model to a free wake model in FAST v6 but validation tests were not completed. The authors have updated this unpublished FAST v6 to FAST v7 with AeroDyn 13. It then combines aerodynamics and hydrodynamics for the floating wind turbine. Firstly the verification test was performed by the free wake model according to NREL VI test. After that the FAST v7 was used in floating wind turbine simulations with three different aerodynamic models.

NUMERICAL SIMULATION

Coupled Free-wake Model

The free-wake model is based on the lifting line theory. The blade is represented by a bound vortex filament. To satisfy the Helmholtz theorem, the bound vortex filament cannot start or end in a flow. Therefore a pair of horseshoe lines is trailing into the downstream field. In the far field, there is a vortex line with equal strength to the bound

vortex which makes the flow a closed ring. When considering the unsteadiness of the flow field, the downstream field can be modeled as a set of vortex lines generating and shedding downward. At every time step, the circulation should follow the Kelvin's theorem.

$$\frac{D\Gamma}{Dt} = 0 \tag{1}$$

Due to the vortex variation along the span, bound vortex is divided into N stations, i=1, 2, ..., N. Considering current step t and previous step t-1, satisfying Eq.1 we can get the shed circulation:

$$\Gamma_{shed}(i,t) = \Gamma_{bound}(i,t) - \Gamma_{bound}(i,t-1) \tag{2}$$

Related to bound circulation gradients, the trailing circulation can be derived from this equation:

$$\Gamma_{trail}(i,t) = \Gamma_{bound}(i,t) - \Gamma_{bound}(i+1,t) \tag{3}$$

Seen from Eqs. 2~3, the bound circulation is the key parameter we must have. The induced velocities on lifting line by the wake points are calculated through the Biot-Savart law. And the bound circulation follows the famous Kutta-Joukowski theorem:

$$L = \rho_\infty V \Gamma_{bound} = \frac{1}{2}\rho_\infty V^2 c c_l \tag{4}$$

The bound circulation can be solved from Eq. 4 via fixed-point iteration.

Considering the bound circulation at current t the same as the one at next step t+1, using an Euler predictor-corrector together with the Biot-Savart law, the position of each wake point at time step t+1 can be predicted. Repeating the steps of calculating new bound circulation the loads on step t+1 can be obtained. The loads are then passed to structural code to do the motion and structure simulation of the whole system. Up till now the aero-hydro coupled procedure is completed in one step. For details of the free vortex theory please see Prof Leishman's book shown in reference (Leishman, 2006).

The velocities from the platform are induced velocities relative to the freestream velocity. Some researchers directly added the FAST calculated platform velocities onto the turbine to discuss the floating wind turbine issue with CFD method or free-wake model (Bahuguni and Sivalingam, 2014; Sebastian, 2012). This is seen as a decoupled method while the method used in this paper is a fully coupled method since the platform induced motions and velocities are calculated each step under the effect of aerodynamic damping.

NREL VI Experiment Description

The NREL Phase VI experiment has been conducted by Hand (Hand et al., 2001) at the NASA Ames 24.4m×36.6m wind tunnel. The blade used in the NREL VI test was both twisted and tapered. From 0.25R to the tip the blade type is uniform corresponding to S809 airfoil. To measure the pressures, 22 pressure taps were mounted on the surface of the blade at five spanwise locations: 0.3R, 0.47R, 0.63R, 0.8R and 0.95R. The NREL VI Sequence S was used to verify the free wake code in steady and 30 ° yaw conditions with 3 ° for the tip pitch angle. The wind turbine and operating conditions are summarized in Table 1.

Table 1. NREL VI wind turbine information and working conditions

	Unit	Value
Number of blades		2
Rotor speed	rpm	72
Rotor diameter	m	10.1
Hub height	m	12.2
Pitch angle	deg	3
Yaw angle	deg	0/30
Free-stream velocity	m/s	5/7/10/13/15/20/25

NREL 5MW Onshore and OC3 Spar-type Wind Turbines

After comparisons through the NREL VI wind turbine, the NREL 5MW onshore and spar-type wind turbines (Jonkman, 2010a, b) are studied as the main part of this paper. The input models are all included in the original FAST v7 pack and Dr Jonkman's website. They are all widely used and studied models. In the OC3 project, only the BEM and GDW were used to do the analysis. It is interesting to see what the results are when using free-wake model as the aerodynamic processor.

As discussed in Dr Sebastian's thesis, the reduced frequency can be used to describe the unsteadiness of the turbine (Sebastian, 2012). The reduced frequency k is defined in Eq. 5, where f is the platform oscillating frequency induced by the wave and c is the chord length.

$$k = \frac{\omega c}{2V} = \frac{\pi f c}{V} \tag{5}$$

For $k > 0.05$, the flow should be considered unsteady (Leishman, 2006). For a moving platform the local velocity of blade section (denominator of reduced frequency) is changing, however Eq. 5 is useful to give the degree of the flow unsteadiness approximately.

Let $k = 0.05$, then we can draw the demarcation curves under different operating conditions using Eq. 6 where U is the wind velocity and Ω is the rotor speed, seen in Fig. 1.

$$f = \frac{0.05}{\pi}\frac{\sqrt{U^2 + (r\Omega)^2}}{c} \tag{6}$$

The oscillating frequency falls in the right of the demarcation curve will introduce unsteadiness to the flow. When working in high tip speed ratio condition (small wind velocity), the wind turbine is more likely to meet the unsteadiness, seen from Fig. 1. And when the wind velocity is small and below rated velocity, the torque-control system is not working. Therefore all the power is determined by the incoming velocity. While it is a steady case in onshore turbine, the moving platform will introduce induced velocities into the rotor and the whole system. The wave frequency is an important parameter to be selected when doing analysis.

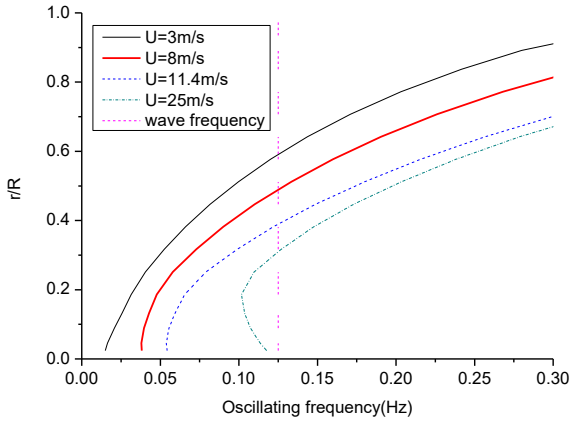

Fig. 1 Demarcation curves for 5MW turbine

In this paper, the wind velocity is fixed to 8m/s. To simplify the problem and to see the main feature of the issue, only linear wave condition was simulated. A linear wave was selected as the severe operating condition with the wave height H=5m and wave period T=8s. When oscillating in this frequency f=1/T=0.125Hz, there will be unsteadiness from the root to the mid-span of the blade, seen from Fig. 1. The torque-control and pitch-control systems in FAST were switched off to let the rotor rotate in constant speed. All unsteady cases were run with Leishman-Beddoes option on.

Floating Case with linear wave: H=5m, T=8s

Seen from demarcation curves in Fig. 1, the high frequency waves introduce more unsteady components into the system. In the ocean, the wave frequencies always fall into the range 0.05~0.2Hz. Only considering the first-order forces, the resulting 6 DOFs induced frequencies are sometimes relatively small to bring strong unsteadiness to the wind turbines comparing to other high frequency oscillations like breaking wave force and structural vibration. But due to the huge size of the tower and blades, small movements in the oscillating frequency may introduce great disturbances in the wind flow area when the effects are translated onto the turbine rotor. In this paper only the unsteadiness introduced by the platform motions are discussed. The main effects from the surge and pitch motions are analyzed.

RESULTS

NREL VI steady conditions

In this section the steady cases for 7 different wind velocities were simulated using BEM, GDW and free wake model in FAST, seen from Table 1. When using free wake model, the time step was set to 0.023s to ensure the azimuth angle increased 10 ° for each step. And the wake generated up to 2 diameters behind the rotor to obtain accurate induced velocities. A helical wake was used as the starting wake and after several seconds the wake would reach the equilibrium condition. To simulate the wind turbine in 40 seconds, it took 2 hours to perform in single core of an Intel i7-2600 3.4GHz PC.

The calculated power and thrust are presented in Fig. 2 and Fig. 3. For the small wind conditions U=5m/s and U=7m/s when the wind turbine is not stall, all the three methods produce good results in both thrust and power. After U=10m/s the turbine is in stalled condition, the discrepancies occur among the three models.

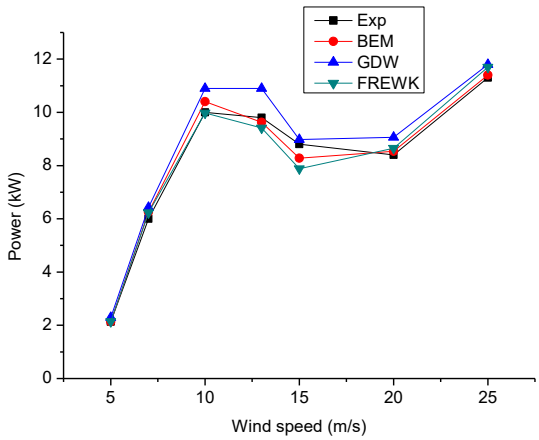

Fig. 2 Comparison of measured and calculated power

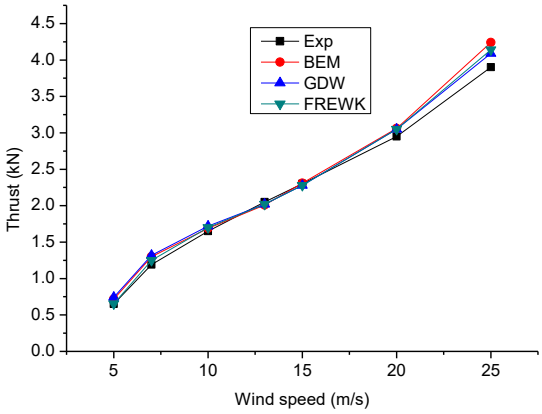

Fig. 3 Comparison of measured and calculated thrust

NREL VI 30 °yaw conditions

The 30 ° yaw cases were performed in U=5m/s and 7m/s conditions where the models provided closer results compared with experimental results. Each case was performed in 40s in which the last 30s were used to get the average aerodynamic force coefficients. Due to page limitation only the normal force coefficients (Cn) and tangential force coefficients (Ct) of case U=7m/s are presented with experimental data, seen from Fig. 4 to Fig. 13.

The free wake model produces close results in different sections comparing to the experimental data. The results from GDW are similar to the ones obtained by free wake model. Comparing to the experimental data, BEM discrepancy gets higher from mid-span to the tip region, seen from Fig. 6 to Fig. 8 and Fig. 11 to Fig. 13. The skewed wake corrections and tip-loss correction in AeroDyn 13 may not be reliable for the BEM to get good result. Recently a new BEM skewed-wake model has been developed by Dr Ning in AeroDyn 15 (Ning, 2015) which produces much better results than the old BEM model in AeroDyn 14. From the AeroDyn changelog there are not any changes made on BEM corrections in AeroDyn 14 comparing with AeroDyn 13. We can infer that BEM with new corrections in AeroDyn 15 could be better than both the BEM in AeroDyn 13 and AeroDyn 14. The results in this paper will be compared with the new AeroDyn 15 BEM model in future study. More validation tests will be performed using

the free wake model according to NREL VI and MEXICO wind turbines in future study. The free wake and GDW also produce better results in U=5m/s case than the BEM model. Seen from the good agreement between the free wake model and experimental data in 30 ° yaw conditions it is encouraging to use it in other unsteady conditions like the floating wind turbine. Meanwhile the GDW can generate reasonable good result comparing with experimental data in yaw cases. Its reliability in floating wind turbine could be further studied together with free wake model.

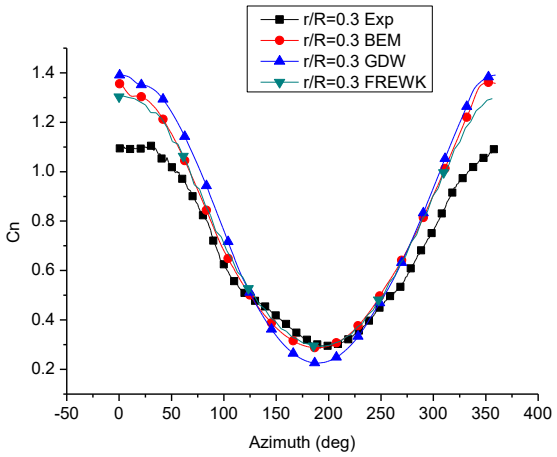

Fig. 4 Normal force coefficient at 0.3R, U=7m/s, Yaw=30 °

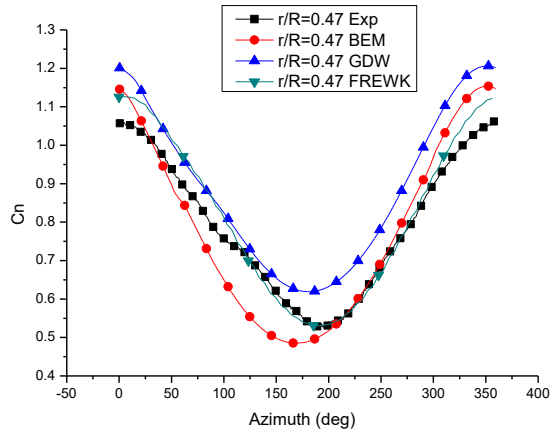

Fig. 5 Normal force coefficient at 0.47R, U=7m/s, Yaw=30 °

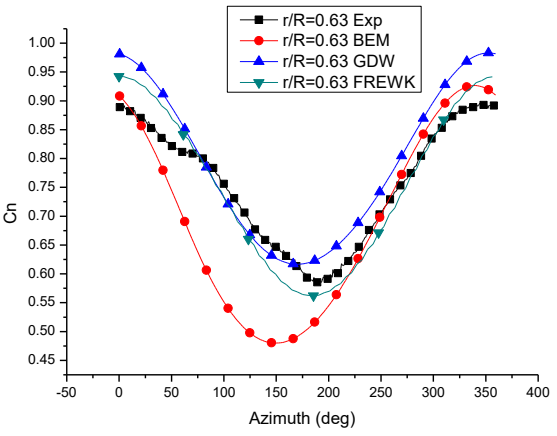

Fig. 6 Normal force coefficient at 0.63R, U=7m/s, Yaw=30 °

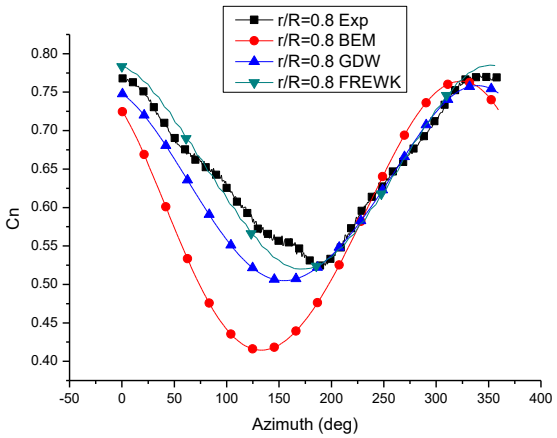

Fig. 7 Normal force coefficient at 0.8R, U=7m/s, Yaw=30 °

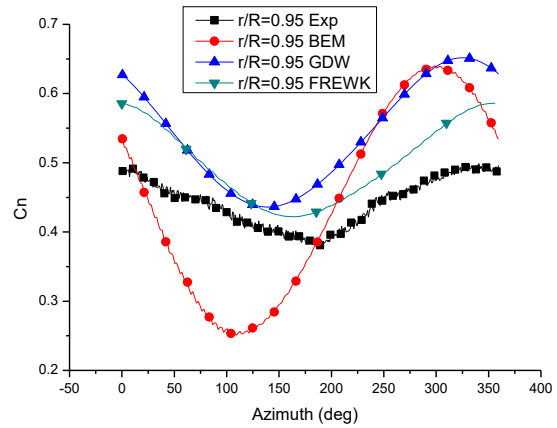

Fig. 8 Normal force coefficient at 0.95R, U=7m/s, Yaw=30 °

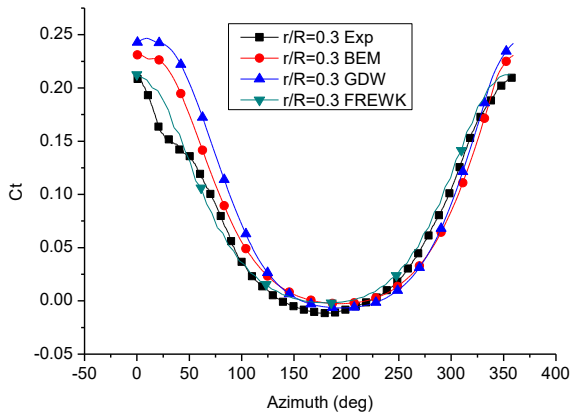

Fig. 9 Tangential force coefficient at 0.3R, U=7m/s, Yaw=30 °

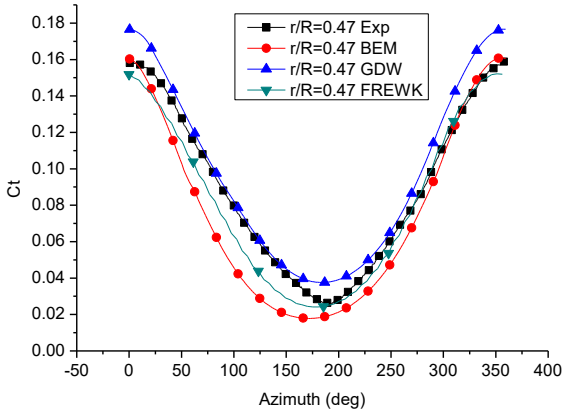

Fig. 10 Tangential force coefficient at 0.47R, U=7m/s, Yaw=30 °

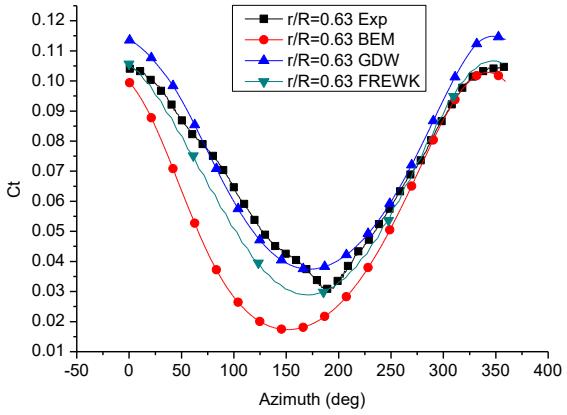

Fig. 11 Tangential force coefficient at 0.63R, U=7m/s, Yaw=30 °

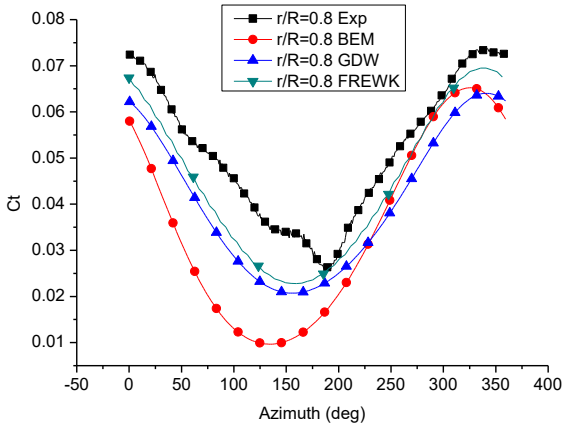

Fig. 12 Tangential force coefficient at 0.8R, U=7m/s, Yaw=30 °

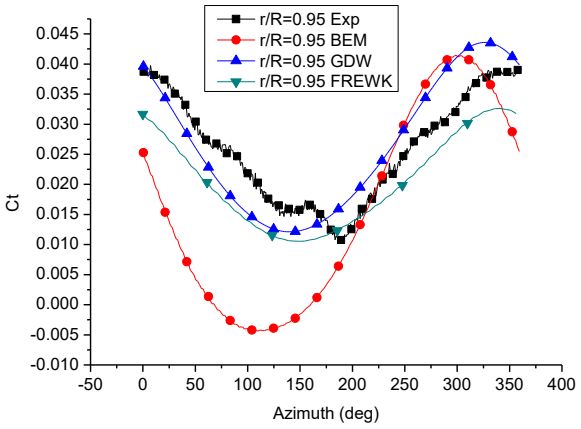

Fig. 13 Tangential force coefficient at 0.95R, U=7m/s, Yaw=30 °

5MW Onshore Wind Turbine

The free-wake model has been performed according to NREL VI experiment previously. It is to be used to simulate the 5MW onshore wind turbine at 8m/s. The wake used for calculating the induced velocity is extended up to 3 diameters distance after the rotor plane. The 5 °azimuth angle per step was used to obtain accurate result.

The global performances rotor thrust and rotor power can be used to evaluate the simulations. It is seen in Fig. 14 that the percentage of thrust discrepancy between BEM and free-wake model is less than 1%. In the rotor power seen from Fig. 15, it reaches 3.6% which is still a reasonable good result. It can be seen that the two dynamic methods free-wake and generalized dynamic wake produce close results. Seen from the angle of attack lines in Fig. 16, the value from free-wake model is approximately 0.2 °higher than the one from the BEM theory along the blade. The GDW result is approximately 0.2 °higher than the one from free wake model from the in-board sections to the mid-span while it decreases a bit from mid-span to tip region. Because of the insufficient treatment of tip loss in AeroDyn's GDW implementation the result from GDW does no match the one from BEM.

The section thrust and torque can be obtained through Eq. 7~8

$$dT = B\frac{1}{2}\rho V_{total}^2\left(C_l\cos\phi + C_d\sin\phi\right)cdr \tag{7}$$

$$dQ = B\frac{1}{2}\rho V_{total}^2\left(C_l\sin\phi - C_d\cos\phi\right)crdr \tag{8}$$

ϕ is the inflow angle which equals to $\theta_{tip}+\theta_{twist}+\alpha$. The angle of attack from 0.4R to R shown in Fig. 16 is around 5 °. There is no tip pitch angle in the U=8m/s condition. And the twist angle decreases from 9 ° to 0 ° from spanwise 0.4R to R. So the inflow angle ϕ is less than 14 °in which the small angle approximation can be used:

$$\sin\phi = \phi \tag{9}$$

$$\cos\phi = 1-\frac{\phi^2}{2} \approx 1 \tag{10}$$

The drag coefficient in is less than 0.01 when angle of attack is below 7 °. So from the mid-span to the tip the thrust and torque factors can be simplified as follows

$$\left(C_l \cos\phi + C_d \sin\phi\right) = C_l \tag{11}$$

$$\left(C_l \sin\phi - C_d \cos\phi\right) = C_l\phi \tag{12}$$

Assume $\phi = 10\,\text{deg}$, a $2\,°$ difference in predicting the angle of attack can cause approximately 20% higher discrepancy in the torque and power value (Eq. 12) than the discrepancy in thrust (Eq.11). So the torque and power of this 5MW wind turbine are more sensitive than the thrust force.

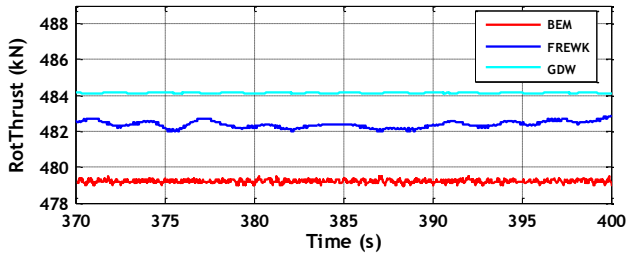

Fig. 14 Rotor thrust of the onshore wind turbine, U=8m/s

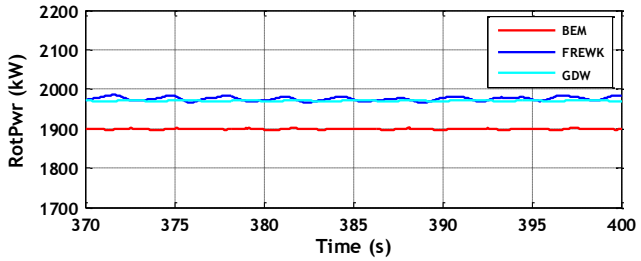

Fig. 15 Rotor power of the onshore wind turbine, U=8m/s

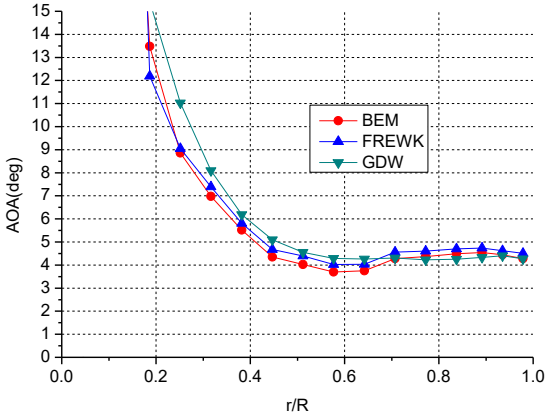

Fig. 16 Angle of attack from BEM and free-wake model, U=8m/s

OC3 Phase IV Case

After comparison through NREL VI wind turbine and 5MW on shore wind turbine it is to be used in floating cases. Unlike the steady cases with fixed induced velocities, when the wind turbine is floating and moving, the induced velocities and angle of attack are changing all the time. When the wind turbine was moving with the linear wave H=5m and T=8s, the only two DOFs surge and pitch were switched on. The induced velocities were only related to these two motions. This can simplify the issue and control the number of variables.

From above discussion we know that the free-wake and GDW derive slightly bigger angle of attack than the BEM method. While the turbine is pitching and surging, the AOA will be becoming bigger or smaller than in the onshore case due to the induced velocities. When the turbine is pitching towards the incoming flow field we define it as pitching forward. The AOA reaches the peak point when the turbine is pitching forward and right in the vertical status. At this time the platform pitch angle is at the mean value and the pitch velocity reaches the highest point in this direction.

In Fig. 17, the results of angle of attack from free-wake model and BEM theory are represented. It is known that the BEM is valid when the induction factor is less than 0.4, after that the turbulent state and vortex ring state occur and the Glauert correction is used for high induction factors in AeroDyn BEM. Seen from Fig. 18, the axial tip induction factor calculated by free wake model is less than 0.4 which is much small than the one from BEM in moving forward motion. The free-wake model gets smaller induction factor when the turbine is pitching forward so with the higher angle of attack at this point (925s), seen from Fig. 17.

The induction factors predicted by the free-wake model are not always smaller than the ones from BEM. When the turbine is pitching backwards, it derives bigger induction factor by the free-wake model. So free-wake resulted angle of attack is smaller than the one from the BEM theory.

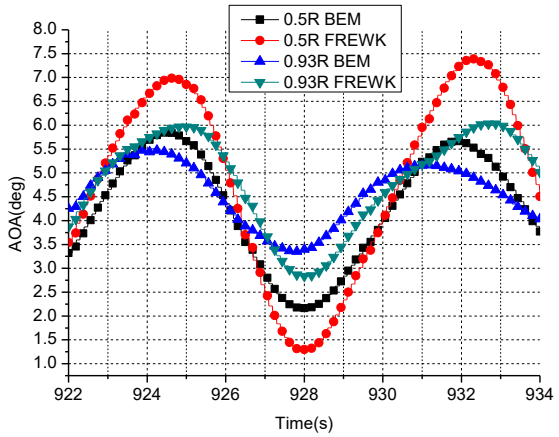

Fig. 17 Angle of attack at blade stations

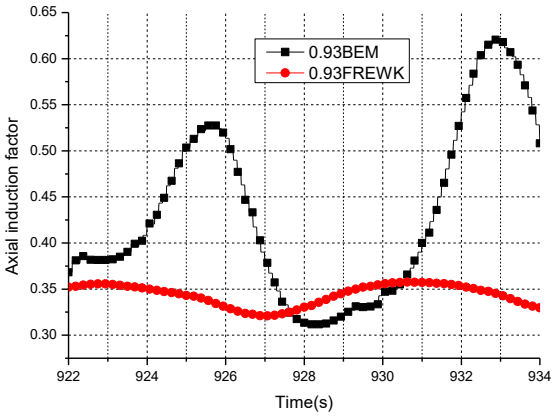

Fig. 18 Axial induction factor at tip

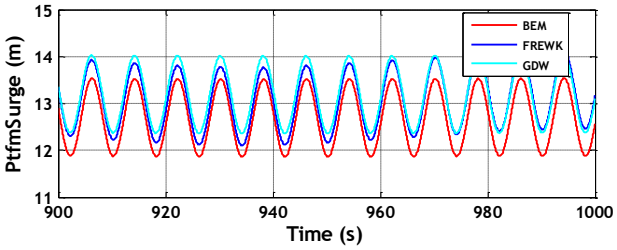

Fig. 19 Platform surge in small scale

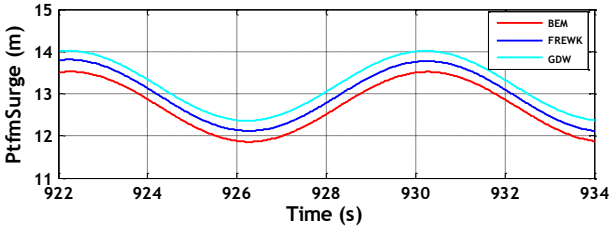

Fig. 20 Platform surge in large scale

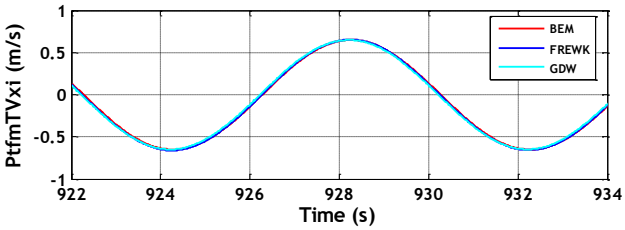

Fig. 21 Platform surge velocity

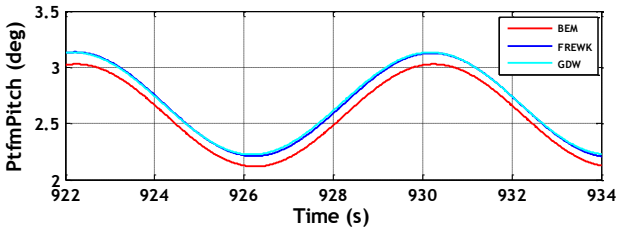

Fig. 22 Platform pitch

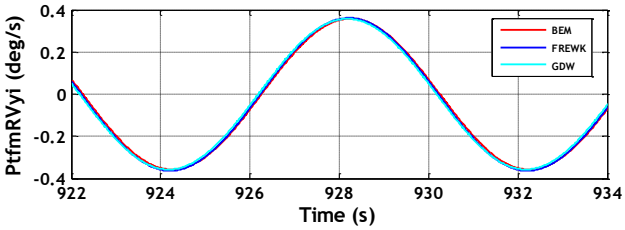

Fig. 23 Platform pitch velocity

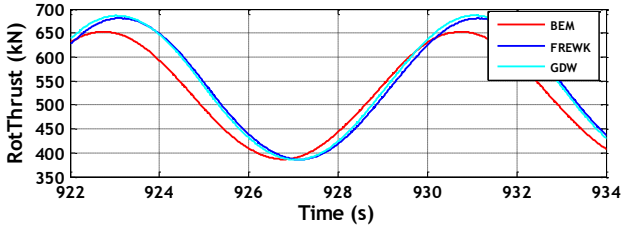

Fig. 24 Rotor thrust of the floating wind turbine

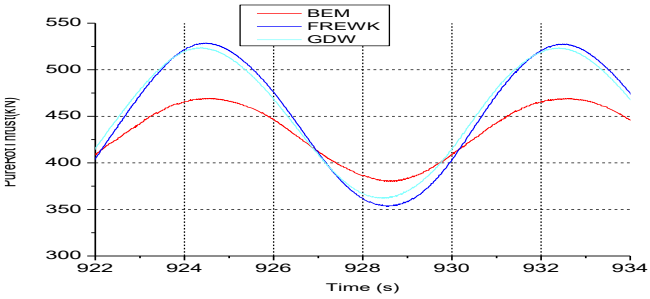

Fig. 25 Pure rotor thrust

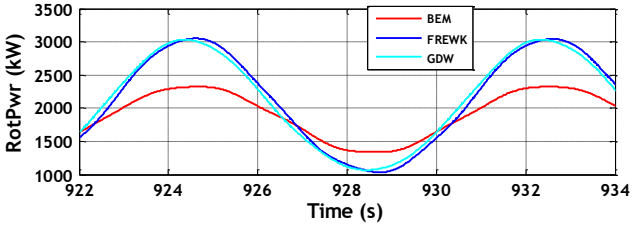

Fig. 26 Rotor power of the floating wind turbine

Although the angles of attack from the two theories are different, the resulted thrust forces have small discrepancy. It has been discussed above that the power is more sensitive than the thrust while power is the most important parameter we want to get in wind turbine industry. The thrust force on the rotor will be translated onto the platform, but due to the design of this platform, the motions of the whole wind turbine system are dominant by the wave forces. The wind force provides an offset on the average positions of surge and pitch motions. It is seen that the average surge and pitch predicted by free-wake and GDW are slightly higher than the ones from BEM theory. But the amplitudes of these motions are the same predicted by three different methods. The surge and pitch velocities are also the same from these three methods. So the difference in angle of attack is only the result by the different ways of calculating induced velocity. The great discrepancy (Fig. 26) when predicting the peak rotor power states that it needs to further evaluate the different methods for the floating wind turbine designing codes.

In this paper, the good agreement between the free-wake model and GDW shows that it is encouraging for the use of GDW to the offshore floating wind turbine simulations because of its low computation cost. As discussed above, the selected induced frequency may not be enough to show strong unsteadiness of the wind turbine. The two theories may derive different results when considering the structural vibration and breaking wave forces on the system. Also in the paper only the global forces and motions are presented, the forces on each section on blade are to be examined between the two different methods.

The motions have been prescribed to a CFD model to simulate the same case by the other researcher in the author's group. The comparison of GDW, free wake and CFD results will be presented in later papers.

CONCLUSIONS

A FAST v6 with free-wake model has been updated to FAST v7 which makes it possible to do the simulation considering both the aerodynamics and hydrodynamics. Through comparison to the NREL VI experimental data the free-wake model and GDW provide good numerical results. The BEM model in AeroDyn 13 can produce good result on steady cases but big discrepancies are found of the aerodynamic loads at the tip region (30 ° yaw). The result on NREL 5MW onshore wind turbine has been compared with BEM, GDW and free wake models in FAST where good agreement is found in this steady condition in all three different models.

In order to analyze the OC3 spar type floating wind turbine, a severe linear wave conditions was chosen to do the simulations. The motions of the floating wind turbine are dominant by the wave forces. The wind force only produces offset on mean position. But by using different aerodynamic method, the percentage of discrepancy in rotor power can reach up to 30% between BEM and the other two dynamic methods. It may not be appropriate to apply the BEM theory in AeroDyn 13 on floating wind turbine simulation in high speed ratio condition without further corrections on this theory. The free-wake model and GDW model could be reliable tools to investigate the complex flow before and after the rotor when the wind turbine is moving. Further studies will be carrying on with CFD simulation, new AeroDyn 15 and experimental tests. And the free wake model will be updated to work with FAST v8 which has superior hydrodynamics modeling capability to FAST v7.

ACKNOWLEDGEMENTS

The authors would like to thank Dr Shan Huang in BP for his great assistance. Prof Hugh Currin, Dr Jason Jonkman and Dr Scott Schreck are kindly acknowledged for their support of the study and experimental data.

REFERENCES

Bülk, M., (2012). "Evaluation of a Lifting Line Free Vortex Wake Method for Wind Turbine Simulation," Thesis written at REpower Systems SE in Osterroenfeld, University of Stuttgart.

Bahuguni, A., Sivalingam, K., (2014). "Implementation of Computational Methods to Obtain Accurate Induction Factors for Offshore Wind Turbines," *Proc. of 33rd International Conference on Ocean, Offshore and Arctic Engineering*, San Francisco, USA.

Currin, H., (2007). "A Dynamic Prescribed Vortex Wake Model for the FAST/AeroDyn Wind Energy Conversion Simulation Code," Ph.D. Thesis, Mechanical Engineering, University of Nevada.

Hand, M.M., Simms, D.A., Fingersh, L.J., et al., (2001). "Unsteady Aerodynamics Experiment Phase VI Wind Tunnel Test Configurations and Available Data Campaigns," TP-500-29955; Golden, CO: National Renewable Energy Laboratory.

Jonkman, J.M., (2010a). "Definition of a 5-MW Reference Wind Turbine for Offshore System Development," NREL/TP-500-28060Golden, CO: National Renewable Energy Laboratory, USA.

Jonkman, J.M., (2010b). "Definition of the Floating System for Phase IV of OC3," NREL/TP-500-47535Golden, CO: National Renewable Energy Laboratory, USA.

Leishman, L.G., (2006). *Principles of Helicopter Aerodynamics*, 2nd ed. Cambridge University Press, New York.

Matha, D., Fischer, S.-A., Hauptmann, S., (2013). "Variations in Ultimate Load Predictions for Floating Offshore Wind Turbine extreme Pitching Motions applying different Aerodynamic Methodologies," *Proceedings of the Twenty-third International Offshore and Polar Engineering*, Anchorage, Alaska, USA.

Ning, S.A., (2015). "Development and Validation of a New Blade Element Momentum Skewed-Wake Model within AeroDyn," *AIAA Science and Technology Forum and Exposition*, Kissimmee, Florida, USA

Quallen, S., ;, Tao, X., Pablo, C., et al., (2014). "CFD Simulation of a Floating Offshore Wind Turbine System Using a Quasi-static Crowfoot Mooring-Line Model," *Journal of Ocean and Wind Energy*, 1 (3), 143-152.

Robertson, A., Jonkman, J.M., Vorpahl, F., et al., (2014). "Offshore Code Comparison Collaboration Continuation within IEA Wind Task 30: Phase II Results Regarding a Floating Semisubmersible Wind System," *Proc. 33rd International Conference on Ocean, Offshore and Arctic Engineering*, San Francisco, USA.

Sant, T., (2007). "Improving BEM-based Aerodynamic Models in Wind Turbine Design Codes," Ph.D. Thesis, Wind Energy Institute, Delft University.

Sebastian, T., (2012). "The Aerodynamics and Near Wake of an Offshore Floating Horizontal Axis Wind Turbine," Ph.D. Thesis, Mechanical and Industrial Engineering, University of Massachusetts Amherst.

van Garrel, A., (2003). "Development of a wind turbine aerodynamics simulation module," ECN-C-03-079; Energy Research Center of the Netherlands, ECN.

Wang, T., (1999). "Unsteady aerodynamic modelling of horizontal axis wind turbine performance," Ph.D. Thesis, Faculty of Engineering, University of Glasgow.